



Contents lists available at ScienceDirect

Bioorganic & Medicinal Chemistry Letters

journal homepage: www.elsevier.com/locate/bmcl

Imidazo[1,2-*a*]pyridine-based peptidomimetics as inhibitors of Akt



Young B. Kim, Chang Won Kang, Sujeewa Ranatunga, Hua Yang, Said M. Sebti, Juan R. Del Valle*

Drug Discovery Department, H. Lee Moffitt Cancer Center and Research Institute, Tampa, FL 33612, USA

ARTICLE INFO

Article history:

Received 9 June 2014

Revised 16 August 2014

Accepted 19 August 2014

Available online 28 August 2014

Keywords:

Kinase inhibitor

Peptide mimic

Dipeptide surrogate

 β -Strand mimic

ABSTRACT

We report the design, synthesis, and biological evaluation of imidazopyridine-based peptidomimetics based on the substrate consensus sequence of Akt, an AGC family serine/threonine kinase hyperactivated in over 50% of human tumors. Our ligand-based approach led to the identification of novel substrate mimetic inhibitors of Akt1 featuring an unnatural extended dipeptide surrogate. Compound **11** inhibits Akt isoforms in the sub-micromolar range and exhibits improved proteolytic stability relative to a parent pentapeptide.

© 2014 Elsevier Ltd. All rights reserved.

The use of peptidomimetics for the inhibition of kinase–substrate interactions is not widely pursued due to the perceived challenges associated with precise topological mimicry, chemical synthesis, and bioavailability. However, the disruption of these interactions holds several potential advantages over ATP-site targeting approaches, including distinct target selectivity and improved therapeutic profiles through inhibition of specific regulatory mechanisms.^{1–3}

Akt (PKB) is one example of a kinase that has been targeted by several different small molecule approaches.^{4–8} Akt is an important regulator of cell growth, cell-cycle progression, transcription and metabolism, and is known to phosphorylate over 20 endogenous substrates.^{5,9–12} Many of these substrates are intimately involved the induction of apoptosis and the arrest of cell proliferation, and are inactivated upon phosphorylation by Akt. Enhanced Akt activity through increased expression, upstream amplification of PI3K, or loss of PTEN, its most important negative regulator, is observed in over 50% of all human solid tumors.^{13–17} Akt has thus emerged as an attractive target for the development of novel anticancer therapeutics.^{4,6,7,18–22}

Most small molecules block Akt activity by direct inhibition of the ATP-binding site, interfering with cellular localization (via inhibition of the Pleckstrin Homology domain), or through allosteric binding. Recently, mimics of the consensus substrate peptide of Akt have also emerged as lead compounds for further development. While achieving ligand complementarity in the relevant protein–protein interaction (PPI) region is expected to be more topochemically demanding, such inhibitors may also exhibit better

selectivity relative to PH and ATP-binding domain antagonists. Early work in this area focused polypeptides exhibiting IC₅₀ values in the low to sub-micromolar range (~10–0.1).^{23–25} A co-crystal structure of Akt1 bound to a substrate peptide in the presence of an ATP-competitive inhibitor revealed that the peptide adopts a highly extended conformation in the binding cleft.²⁶ Efforts to reduce peptide character while maintaining the bioactive conformation have led to the identification of additional pseudosubstrate Akt1 inhibitors.^{27–31}

Our group recently reported inhibitors of Akt1 based on a consensus sequence incorporating an azabicycloalkane dipeptide surrogate.³⁰ Here, we describe the design and synthesis of a series of imidazopyridine-based peptidomimetics with enhanced potency and proteolytic stability. The undecapeptide Akt substrate GRPRTSSFAEG (Crosstide) was used as a lead structure and the central Thr7–Ser8 dipeptide was identified as a candidate site for conformational constraint (Fig. 1).

The general synthesis of Akt substrate mimics is depicted in Scheme 1. The imidazo[1,2-*a*]pyridine (IP)-based dipeptide surrogate³² was prepared by bromination of β -ketoester **1** and subsequent condensation with 2,3-diaminopyridine. Amidation of the IP N-terminus with protected amino acids required stirring in the presence of EDC in DCM for 24–48 h for optimal yields. The addition of auxiliary base or the use of other common coupling conditions (HBTU/HOBt, HATU, PyBOP, COMU, DEPBT) resulted in significantly lower conversion. The slow rate of amidation also precluded direct coupling to various N-protected arginine derivatives, all of which underwent intramolecular cyclization prior to reacting with the IP amine. In contrast, **2** was efficiently coupled to Cbz-Orn(Boc)-OH, Cbz-Lys(Boc)-OH, and Cbz-Har(Boc)₂-OH without any observable lactam formation. Arginine derivatives were

* Corresponding author.

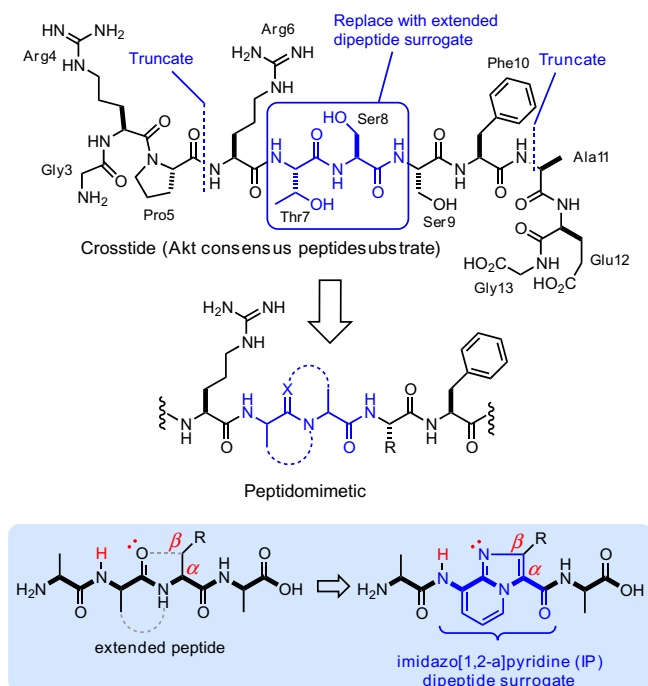
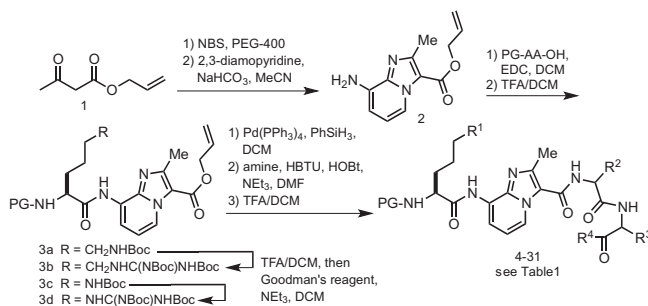


Figure 1. Design of peptidomimetic Akt inhibitors.



Scheme 1. Synthesis of imidazo[1,2-a]pyridine-based inhibitors.

prepared via Boc acidolysis and subsequent guanidinylation using Goodman's reagent to give protected tripeptide mimics **3b** and **3d**.

Incorporation of various C-terminal fragments was achieved by removal of the allyl ester protecting group and condensation with amino acid and dipeptide derivatives. Notably, the dipeptide amides used in the condensation reaction were efficiently prepared by simple aminolysis of the corresponding Boc-protected dipeptide methyl esters (see [Supplementary data](#)). We found this procedure to be a convenient and racemization-free method to produce a variety of protected peptide amides. After coupling to the IP-containing fragment, Boc group removal with TFA/DCM was followed by column chromatography to afford inhibitors **4–31**.

All compounds were assayed *in vitro* for their ability to inhibit the phosphorylation of Crosstide by Akt1 in the presence of 10 μ M 33 P-labeled ATP (dose-response experiments were repeated 3 times, and IC_{50} values and 95% confidence intervals were calculated based on a variable slope four parameter model). As shown in [Table 1](#), truncation of the lead substrate down to tetrapeptide mimics **4–7** afforded compounds with no appreciable Akt1 inhibitory activity at 20 μ M. Pentapeptide mimic **8**, which incorporates the native Ser9-Phe10 motif was also inactive *in vitro*. Replacement of Ser9 (native phosphorylation site) with the more hydrophobic Leu (**9**) or Phe (**10**) residues led to a dramatic increase

in potency against Akt1. Optimal potency against Akt1 (IC_{50} = 0.64 μ M) was achieved with derivative **11**, which incorporates a Val-Phe-NHBn C-terminal dipeptide subunit.

In order to obtain preliminary SAR for peptidomimetic **11**, we prepared analogs **12–16**, in which pharmacophores were iteratively deleted. In general, these deletions were not well tolerated and resulted in a significant (>30-fold) loss of potency. The activity of compound **11** was also found to be remarkably sensitive to the incorporation of D-Val or D-Phe residues as in **17** and **18**.

We next prepared a series of side chain analogs to determine optimal pharmacophores within **11**. Derivatives **19–21** harbor an N-terminal Orn, Lys, or Har residue, preserving the important basic pharmacophore at position 6 of the substrate consensus sequence. Orn and Lys side chain analogs **19** and **20** showed slightly weaker potency against Akt1, while the guanidine (Har)-containing analog **21** exhibited an IC_{50} of 1.06 μ M. Phe10-mutated variants **22–24**, also inhibited Akt1 with IC_{50} values in the 1–2 μ M range. Benzyl ester **25** displayed significantly weaker inhibition of Akt1 relative to **11**. As in the case of methyl amide **16**, methyl ester **26** showed no significant activity at 20 μ M concentration. However, other more hydrophobic substitutions at the C-terminus of **11** were well tolerated, with *i*-Bu derivative **29** displaying almost equivalent potency *in vitro*. Attempts to constrain the C-terminal backbone as in **30** and **31** had a deleterious effect on activity.

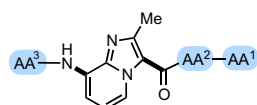
In order to confirm the ability of **11** to block the phosphorylation of the Akt substrate peptide, we employed a non-radioactivity based secondary assay using Akt from cell lysates. HEK293 cells were thus transfected with Myc-tagged Akt1 and the protein was immunoprecipitated using anti-Myc antibody. Incubation of the immobilized enzyme with a substrate GSK3 β fusion protein in the presence or absence of inhibitors was followed by detection of p-GSK3 β by immunoblots. As shown in [Figure 2](#), the control Akt inhibitor MK2206 completely blocks phosphorylation of GSK3 β at 5 μ M. Our substrate mimetic inhibitor, **11**, significantly inhibits p-GSK3 β at concentrations above 1 μ M relative to DMSO control. The approximate IC_{50} value for **11** observed by immunoblots (between 0.3 and 3 μ M) was in good agreement with that obtained in the 33 P-ATP kinase assay above.

Given that **11** was designed to mimic the consensus substrate sequence of Akt, we anticipated that it would show significant activity against each of the Akt isoforms. When evaluated against Akt2 and Akt3 *in vitro*, **11** exhibited IC_{50} values of 0.76 and 0.13 μ M, respectively ([Fig. 3](#)). We also tested compound **11** against seven AGC kinase family members in the hotspot assay to provide preliminary selectivity information. At 10 μ M concentration **11** exhibited less than 50% inhibition of PDK1, PKC α , LATS1, ROCK1, and RSK1. The activity of PKA and MSK1 were inhibited 54% and 65%, respectively, by **11** (see [Supporting information](#)). These data points were obtained using a concentration of **11** 15-fold greater than its Akt1 IC_{50} value, suggesting that the lead inhibitor is moderately selective against closely related kinase targets.

To gain insight into the potential interaction between Akt1 and **11** we performed computational docking experiments with the crystal structure of Akt1 bound to a GSK3 β substrate peptide in the presence AMP-PNP (pdb 106K). An RMSD of 0.51 Å was observed upon self-docking of the substrate peptide using the GLIDE XP protocol. Docking of compound **11** revealed good overlap with the backbone and side chain geometries of Arg6, Ser9, and Phe10 in the native ligand ([Fig. 4](#)). Important hydrogen bonding interactions with Gly312, Glu279, and Glu236 in Akt1 are also maintained in the docked structure of **11**.

Although peptides represent useful starting points for the development of kinase inhibitors, their susceptibility to proteolytic degradation remains a major drawback. To determine the impact of the IP dipeptide surrogate on compound stability, we synthesized the fully peptidic analog of **11** (Cbz-Arg-Thr-Ser-Val-Phe-NHBn) and

Table 1
Structure–activity relationships for compounds **4–31**



Compound	AA ³	AA ²	AA ¹	Akt1 IC ₅₀ (μM)	95% CI (μM)
4	Cbz-Arg	Val-NHBn	—	>20	—
5	Cbz-Arg	Val-OBn	—	>20	—
6	Cbz-Arg	Hyp(Bn)-OBn	—	>20	—
7	Cbz-Arg	pip(N-Bz)	—	>20	—
8	Cbz-Arg	Ser	Phe-NHBn	>20	—
9	Cbz-Arg	Leu	Phe-NHBn	1.59	1.43–1.78
10	Cbz-Arg	Phe	Phe-NHBn	1.13	1.03–1.24
11	Cbz-Arg	Val	Phe-NHBn	0.64	0.55–0.74
12	Moc-Arg	Val	Phe-NHBn	>20	—
13	Cbz-Ala	Val	Phe-NHBn	>20	—
14	Cbz-Arg	Ala	Phe-NHBn	>20	—
15	Cbz-Arg	Val	Ala-NHBn	>20	—
16	Cbz-Arg	Val	Phe-NHMe	>20	—
17	Cbz-Arg	(D)Val	Phe-NHBn	>20	—
18	Cbz-Arg	Val	(D)Phe-NHBn	>20	—
19	Cbz-Orn	Val	Phe-NHBn	3.06	2.17–4.33
20	Cbz-Lys	Val	Phe-NHBn	1.92	1.72–2.15
21	Cbz-Har	Val	Phe-NHBn	1.06	0.95–1.20
22	Cbz-Arg	Val	Phg-NHBn	1.53	1.29–1.82
23	Cbz-Arg	Val	(4-F)Phe-NHBn	2.00	1.65–2.43
24	Cbz-Arg	Val	HomoPhe-NHBn	1.59	1.38–1.83
25	Cbz-Arg	Val	Phe-OBn	5.27	4.78–5.80
26	Cbz-Arg	Val	Phe-OMe	>20	—
27	Cbz-Arg	Val	Phe-NH(4-F)Bn	0.83	0.53–1.30
28	Cbz-Arg	Val	Phe-NH(4-Me)Bn	1.02	0.83–1.25
29	Cbz-Arg	Val	Phe-NHi-Bu	0.67	0.57–0.79
30	Cbz-Arg	Val	Tic-NHBn	>20	—
31	Cbz-Arg	Val	(N-Me)Phe-NHBn	>20	—

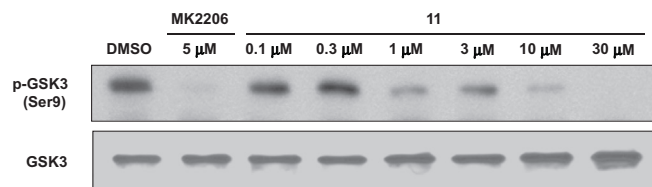


Figure 2. Phosphorylation of GSK3β fusion protein by Myc-tagged Akt1 immunoprecipitated from cell lysates.

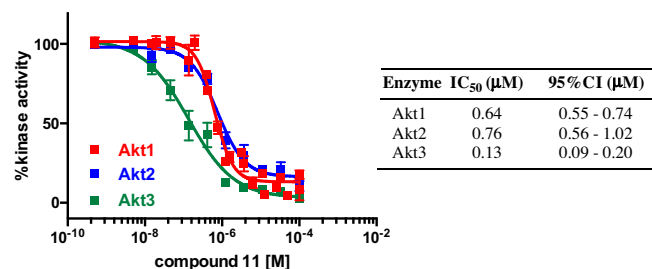


Figure 3. In vitro inhibition of Akt isoforms by **11**.

subjected both compounds to time-course digestion experiments with chymotrypsin and pronase. The imidazopyridine-based peptidomimetic **11** was considerably more stable toward digestion than the control peptide over 48 h at 37 °C (Fig. 5). Crosstide was likewise degraded within 0.5 h upon incubation with either protease (data not shown).

In summary, we have described a ligand-based approach toward the discovery of novel substrate mimetic inhibitors of

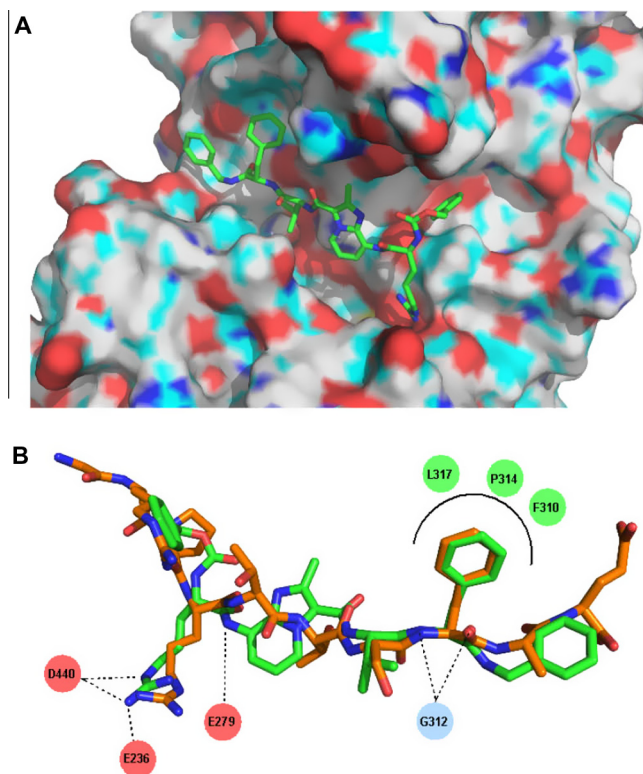


Figure 4. (A) Binding of compound **11** to Akt1 (pdb 106K) as determined by GLIDE XP docking. (B) Overlay of docked conformation of **11** (green) with the bound X-ray conformation of a substrate peptide (orange). Key interactions of **11** with Akt1 are shown.

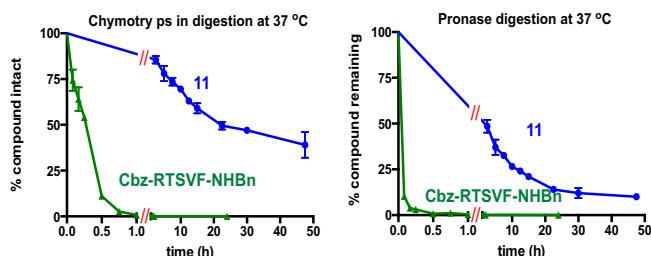


Figure 5. Proteolytic degradation of **11** and a parent pentapeptide.

Akt. These pentapeptide mimics are based on a bicyclic aromatic core structure that was recently developed as a versatile dipeptide surrogate.³² We have previously shown that imidazo[1,2-*a*]pyridine scaffolds can promote an extended conformation when incorporated into peptidic host structures. Substitution of the Thr7-Ser8 dipeptide in Crosside with this motif led to the identification of lead inhibitor **11**, which inhibits Akt-mediated GSK3 β phosphorylation with an IC₅₀ of 0.64 μ M. Compound **11** also displays enhanced stability toward proteolytic degradation relative to its parent peptides. Efforts to further optimize **11** in the pursuit of substrate mimetic Akt inhibitors suitable for in vivo applications are currently underway.

Acknowledgments

This work was supported by the National Institutes of Health (R21CA167215) and by the Anna Valentine Cancer Fund (FIG award). We gratefully acknowledge the Moffitt Chemical Biology Core, Molecular Modeling Unit (NIH P30CA76292) for performing computational docking of compound **11**.

Supplementary data

Supplementary data (experimental procedures and copies of ¹H NMR spectra for compounds **4–31**) associated with this article can be found, in the online version, at <http://dx.doi.org/10.1016/j.bmcl.2014.08.040>.

References and notes

- Arkin, M. R.; Whitty, A. *Curr. Opin. Chem. Biol.* **2009**, *13*, 284.
- Bogoyevitch, M. A.; Fairlie, D. P. *Drug Discovery Today* **2007**, *12*, 622.
- Kirkland, L. O.; McInnes, C. *Biochem. Pharmacol.* **2009**, *77*, 1561.
- Barnett, S. F.; Bilodeau, M. T.; Lindsley, C. W. *Curr. Top. Med. Chem.* **2005**, *5*, 109.
- Cheng, J. Q.; Lindsley, C. W.; Cheng, G. Z.; Yang, H.; Nicosia, S. V. *Oncogene* **2005**, *24*, 7482.
- Collins, I. *Anti-Cancer Agent Med. Chem.* **2009**, *9*, 32.
- Garcia-Echeverria, C.; Sellers, W. R. *Oncogene* **2008**, *27*, 5511.
- Kumar, C. C.; Madison, V. *Oncogene* **2005**, *24*, 7493.
- Staal, S. P. *Proc. Natl. Acad. Sci. U.S.A.* **1987**, *84*, 5034.
- Staal, S. P.; Hartley, J. W.; Rowe, W. P. *Proc. Natl. Acad. Sci. U.S.A.* **1977**, *74*, 3065.
- Bellacosa, A.; Testa, J. R.; Staal, S. P.; Tsichlis, P. N. *Science* **1991**, *254*, 274.
- Du, K.; Tsichlis, P. N. *Oncogene* **2005**, *24*, 7401.
- Altomare, D. A.; Testa, J. R. *Oncogene* **2005**, *24*, 7455.
- Hsu, J. H.; Shi, Y.; Hu, L.; Fisher, M.; Franke, T. F.; Lichtenstein, A. *Oncogene* **2002**, *21*, 1391.
- Zinda, M. J.; Johnson, M. A.; Paul, J. D.; Horn, C.; Konicek, B. W.; Lu, Z. H.; Sandusky, G.; Thomas, J. E.; Neubauer, B. L.; Lai, M. T.; Graff, J. R. *Clin. Cancer Res.* **2001**, *7*, 2475.
- Page, C.; Lin, H. J.; Jin, Y.; Castle, V. P.; Nunez, G.; Huang, M.; Lin, J. *Anticancer Res.* **2000**, *20*, 407.
- Crowell, J. A.; Steele, V. E.; Fay, J. R. *Mol. Cancer Ther.* **2007**, *6*, 2139.
- Bellacosa, A.; de Feo, D.; Godwin, A. K.; Bell, D. W.; Cheng, J. Q.; Altomare, D. A.; Wan, M.; Dubeau, L.; Scambia, G.; Masciullo, V.; Ferrandina, G.; Benedetti Panici, P.; Mancuso, S.; Neri, G.; Testa, J. R. *Int. J. Cancer* **1995**, *64*, 280.
- Cheng, J. Q.; Godwin, A. K.; Bellacosa, A.; Taguchi, T.; Franke, T. F.; Hamilton, T. C.; Tsichlis, P. N.; Testa, J. R. *Proc. Natl. Acad. Sci. U.S.A.* **1992**, *89*, 9267.
- Heering, D. A.; Safonov, I. G.; Verma, S. K. *Annu. Rep. Med. Chem.* **2007**, *42*, 365.
- Li, Q. *Expert Opin. Ther. Pat.* **2007**, *17*, 1077.
- Lindsley, C. W.; Zhao, Z.; Leister, W. H.; Robinson, R. G.; Barnett, S. F.; Defeo-Jones, D.; Jones, R. E.; Hartman, G. D.; Huff, J. R.; Huber, H. E.; Duggan, M. E. *Bioorg. Med. Chem. Lett.* **2005**, *15*, 761.
- Litman, P.; Ohne, O.; Ben-Yaakov, S.; Shemesh-Darvish, L.; Yechezkel, T.; Salitra, Y.; Rubnov, S.; Cohen, I.; Senderowitz, H.; Kidron, D.; Livnah, O.; Levitzki, A.; Livnah, N. *Biochemistry* **2007**, *46*, 4716.
- Luo, Y.; Smith, R. A.; Guan, R.; Liu, X.; Klinghofer, V.; Shen, J.; Hutchins, C.; Richardson, P.; Holzman, T.; Rosenberg, S. H.; Giranda, V. L. *Biochemistry* **2004**, *43*, 1254.
- Obata, T.; Yaffe, M. B.; Lepar, G. G.; Piro, E. T.; Maegawa, H.; Kashiwagi, A.; Kikkawa, R.; Cantley, L. C. *J. Biol. Chem.* **2000**, *275*, 36108.
- Yang, J.; Cron, P.; Thompson, V.; Good, V. M.; Hess, D.; Hemmings, B. A.; Barford, D. *Mol. Cell* **2002**, *9*, 1227.
- Freeman, N. S.; Tal-Gan, Y.; Klein, S.; Levitzki, A.; Gilon, C. *J. Org. Chem.* **2011**, *76*, 3078.
- Kayser, K. J.; Glenn, M. P.; Sebt, S. M.; Cheng, J. Q.; Hamilton, A. D. *Bioorg. Med. Chem. Lett.* **2007**, *17*, 2068.
- Kayser-Bricker, K. J.; Glenn, M. P.; Lee, S. H.; Sebt, S. M.; Cheng, J. Q.; Hamilton, A. D. *Bioorg. Med. Chem.* **2009**, *17*, 1764.
- Ranatunga, S.; Del Valle, J. R. *Bioorg. Med. Chem. Lett.* **2011**, *21*, 7166.
- Tal-Gan, Y.; Hurevich, M.; Klein, S.; Ben-Shimon, A.; Rosenthal, D.; Hazan, C.; Shalev, D. E.; Niv, M. Y.; Levitzki, A.; Gilon, C. *J. Med. Chem.* **2011**, *54*, 5154.
- Kang, C. W.; Sun, Y.; Del Valle, J. R. *Org. Lett.* **2012**, *14*, 6162.